SCIENCE CHINA
Chemistry

• ARTICLES •

September 2010 Vol.53 No.9: 2019–2025
doi: 10.1007/s11426-010-4071-3

Formation of nanotubes and secondary assemblies of cyclodextrins induced by BBOT

ZHANG JingJing, SHEN XingHai*, WU AiHua, ZHANG ChunFen, CHEN QingDe & GAO HongCheng

Beijing National Laboratory for Molecular Sciences; Radiochemistry and Radiation Chemistry Key Laboratory of Fundamental Science; College of Chemistry and Molecular Engineering, Peking University, Beijing 100871, China

Received May 24, 2010; accepted June 16, 2010

The study of cyclodextrin nanotubes is a significant topic among the self-assembly behaviors of cyclodextrins. We report herein the interaction of 2,5-bis(5′-*tert*-butyl-2-benzoxazoyl)thiophene (BBOT) with α-, β-, γ-cyclodextrins (CDs). It has been discovered that the reaction patterns of BBOT with CDs are remarkably different. α-CD forms a simple inclusion complex with BBOT in a stoichiometry of 1:2 (guest:host). β-CD forms a 1:1 inclusion complex with BBOT at its low concentration. At higher concentration of BBOT, the nanotube and secondary assembly of β-CD are formed. As for γ-CD, the nanotube and secondary assembly are formed within the whole concentration range of BBOT studied. The structure of γ-CD nanotubes is different from that of β-CD nanotubes to a certain extent.

BBOT, cyclodextrin, nanotube, secondary assembly

1 Introduction

Cyclodextrins (CDs) are a family of cyclic oligosaccharides composed of α-(1,4) linked glucopyranose units. In this family, α-, β- and γ-CD are the most common cycloamyloses, which have six, seven, and eight glucose units, respectively. With special structures of the hydrophobic inner cavity and hydrophilic outer surface, CD is one of the most significant host molecules in supramolecular chemistry. A large number of novel, ordered supramolecular materials [1–3] as well as rotaxane [4], polyrotaxane [5], catenane [6], molecular necklaces [7] and other supramolecular assemblies have been constructed. Among all of these, the study of CD nanotubes has attracted great attention [8–10].

Common CD nanotubes are assemblies, where two adjacent CDs are associated by non-covalent bonds. "Janus" CDs, which exhibit charge localization of opposite signs at two rims, can build up nanotubes, dimers and trimers in aqueous solutions [11]. Through potential-controlled adsorption technology, Ohira *et al*. constructed nanotube structures of α-, β-, and γ-CDs onto Au (Ⅲ) surfaces [12]. Cyclodextrin nanotubes can also be induced by organic molecules. Agbaria *et al.* discovered that the 2,5-dipheyloxazole (PPO) molecule could lead to the formation of a coaxial array of γ-CD beads in aqueous solutions [13]. Later, they found 2,5-diphenyl 1,3,4-oxadiazole (PPD), 2-phenyl-5-(4-diphenyl)1,3,4-oxadiazole (PBD) and 2,5-(4,4′-diphenyl) 1,3,4-oxazole (BBOD) could also induce the formation of γ-CD nanotubes [14]. Li *et al.* reported the formation of rigid molecular nanotube aggregates of β-CD and γ-CD through linkages by the rodlike molecules of all-*trans*-1,6-diphenyl-1,3,5-hexatriene (DPH). The visualized images of nanotubes were obtained with STM for the first time [15]. The study of the formation of CD nanotubes in the presence of some other organic molecules becomes a subject of great interest [16–25].

Our research group is interested in studies concerning the

*Corresponding author (email: xshen@pku.edn.cn.)

formation of CD nanotubes induced by organic molecules and aims to find out what kinds of organic molecules cause the formation of CD nanotubes. We have found that butyl-PBD [26], 2,2′-biquinoline (BQ) [27], 1,1′-(methylenedi-1,4-phenylene)bismaleimide (MDP-BMI) [27], 4,4′-bis(2-benzoxaolyl)stilbene (BOS) [28], *N,N*′-diphenylbenzidine (DPB) [29] and 2,2′-*p*-phenylenebis(5-phenyloxazole) (POPOP) [30] can induce CDs to form nanotubes and PBD can also induce the formation of β-CD nanotubes [26, 31]. The fact that nanotubes could assembly further to form rod-like structures was discovered for the first time [29, 31] and the concept of secondary assembly was suggested accordingly [31]. Recently, it was reported that *trans*-2-[4-(dimethylamino)styryl]benzothiazole (DMASBT) could induce the formation of β-CD nanotubes and their secondary assembly [32, 33], which further confirmed the viewpoint of us [29, 31]. However, only a small amount of molecules has been discovered to induce CDs to form secondary assembly.

In this work, we studied the different interaction patterns between 2,5-bis(5′-*tert*-butyl-2-benzoxazoyl)thiophene (BBOT) (as shown in Figure 1) and α-, β-, γ-CD. Except for the absorption and fluorescence spectroscopy, fluorescence microscopy, transmission electron microscopy (TEM) and dynamic light scattering (DLS) were used to characterize the cyclodextrin nanotubes. The effect of pH on nanotubes and secondary assembly was also studied. BBOT is a commonly used material for charge transfer and has been applied in OLED [34, 35]. Therefore, the study of the formation of nanotubes and secondary assembly induced by BBOT is of great significance and has potential applications in OLED.

2 Experimental

BBOT (Acros, 99%), α-CD (Acros, 98%+) and γ-CD (Acros, 99%) were used as received. β-CD (Beijing Aoboxing, China) was triply recrystallized from tridistilled water. All the other chemical reagents used in this study were of analytical grade.

In order to prepare CD inclusion complexes and nanotubes, the following procedures were performed: (1) a stock solution of BBOT was prepared in ethanol and an aliquot of the stock solution of BBOT was added to a volumetric flask, with the volume of the stock solution added being no more than 1%; (2) the required amount of CDs was added to the solution; (3) tridistilled water was added to dilute the solution to a certain concentration; (4) the above mixture was sonicated for 1 h, and then incubated for one night before any measurement.

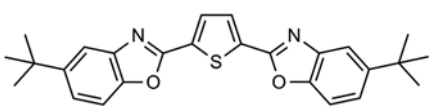

Figure 1 The structure of BBOT.

Absorption spectra were recorded on a U-3010 (Hitachi) spectrophotometer and the slit width was 2 nm. Steady state fluorescence and fluorescence anisotropy were measured on an F-4500 (Hitachi) spectrophotometer. The value of fluorescence anisotropy (r) was obtained by taking the average value for three times. The error was estimated to be as high as 0.005. Fluorescence lifetime measurements were carried out on a fluorescence lifetime spectrometer LifeSpec-Red (Edinburgh). 5000 counts were collected for each sample. Fluorescence images were obtained with a fluorescence microscope IX70-142 (Olympus). Micrographs of TEM were recorded with a JEM-100CX II and high-resolution TEM (F30, Tecnai; H9000, Hitachi) by the negative staining method. Uranyl acetate solution (2%) was used as the staining agent to make the TEM images more clear. DLS measurements were performed on an ALV/DLS/SLS-5022F photo correlation spectrometer. The wavelength of laser was 632.8 nm and the scattering angle was 90°. The samples were treated with 0.2 μm filters (Membrana, micro PES) before the DLS measurements. Density of the solution was measured with a density meter (Mettler Toledo).

3 Results and discussion

3.1 Absorption and steady state fluorescence spectra

As shown in Figures 2(a) and (b), the maximum absorption wavelengths for BBOT in pure water and in aqueous solutions of α-, β-, γ-CD are 358, 358, 375 and 362 nm, respectively. The maximum emission wavelengths are 447, 446, 434 and 498 nm, respectively. This indicates that the microenvironments of the molecule in pure water and in aqueous solutions of α-, β-, γ-CD are different. Therefore, the interaction patterns of BBOT with CDs may also be different.

3.1.1 The interaction of BBOT with α-CD

Figure 3(a) shows fluorescence spectra of BBOT in aqueous solutions of α-CD at various concentrations. The fluorescence intensity of BBOT increases and a small blue-shift occurs on going from water to aqueous solutions of α-CD, which indicates that BBOT moves from water to a less aqueous site and an inclusion complex might be formed. To estimate the association constants and stoichiometries of the inclusion complex, different models of complexation can be considered [36–39]. In this case, reasonable results can be obtained only when the model of 1:2 inclusion complexation is applied, which is based on the following equation:

$$I = \frac{I_0 + I_2 K_2 [\mathrm{CD}]^2}{1 + K_2 [\mathrm{CD}]^2} \quad (1)$$

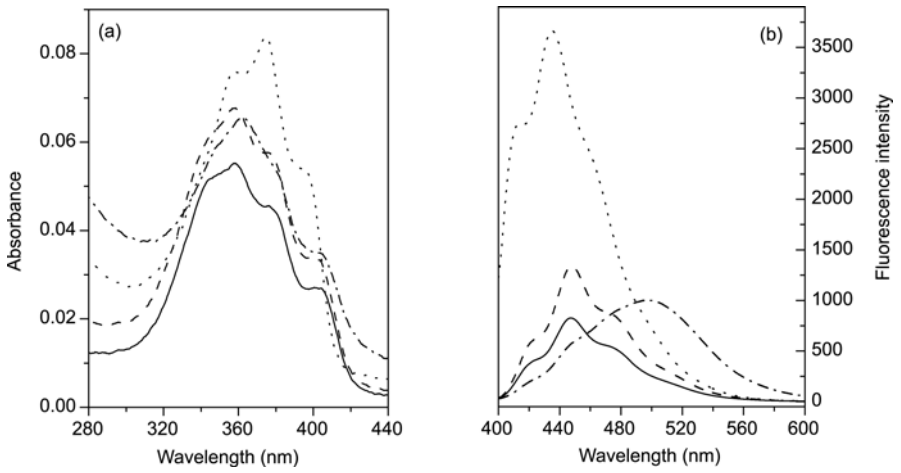

Figure 2 Absorption (a) and fluorescence (b) spectra of BBOT in pure water (solid line) and in aqueous solutions of α-CD (dashed line), β-CD (dotted line), and γ-CD (dash-dot line) ([BBOT] = 2×10^{-6} M, [CD] = 10 mM).

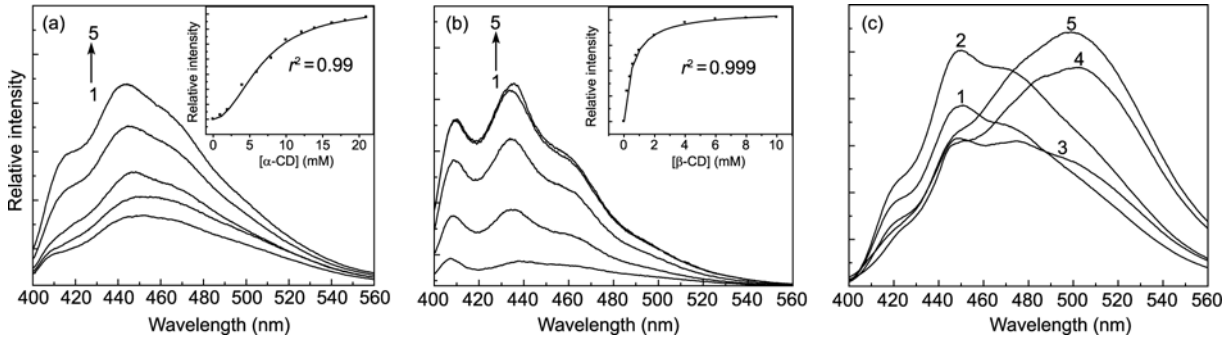

Figure 3 Fluorescence spectra of BBOT in CDs. (a) [BBOT] = 2×10^{-6} M, from 1 to 5, [α-CD] = 0, 2, 6, 10, 20 mM. The inset shows the relative fluorescence intensity (λ = 446 nm) vs. [α-CD]. (b) [BBOT] = 1×10^{-8} M, from 1 to 5, [β-CD] = 0, 0.2, 1, 4, 10 mM. The inset shows the relative fluorescence intensity (λ = 434 nm) vs. [β-CD]. (c) [BBOT] = 2×10^{-6} M, from 1 to 5, [γ-CD] = 0.1, 0.2, 2, 6, 10 mM.

where I_0 and I_2 are fluorescence intensities of BBOT in pure water and the 1:2 inclusion complex, respectively, while K_2 is the association constant of the 1:2 inclusion complex, [CD] represents the equilibrium concentration of CD, which can be replaced by the initial concentration [37]. The value of K_2 is estimated to be $(2.18 \pm 0.16) \times 10^4$ M^{-2} (see Figure 3(a) and the inset).

The fluorescence anisotropy of BBOT in aqueous solutions of α-CD at different concentrations was measured. Upon the addition of α-CD, the r value of BBOT increases slightly. However, the r value hardly increases along with continuous addition of α-CD, which indicates the formation of a simple complex between BBOT and α-CD. The inclusion complexes cannot be linked together and form nanotubes due to the comparatively small cavity of α-CD.

3.1.2 The interaction of BBOT with β-CD

The interaction pattern of BBOT with β-CD depends on the concentration of BBOT. It was found that when the concentration of BBOT is lower than 5×10^{-8} M, reasonable results can be obtained only when the model of 1:1 inclusion complex is considered (see Figure 3(b) and the inset). The association constant K_1 is estimated to be $(1.77 \pm 0.04) \times 10^3$ M^{-1} on the basis of the following equation:

$$I = \frac{I_0 + I_1 K_1 [\mathrm{CD}]}{1 + K_1 [\mathrm{CD}]} \quad (2)$$

where I_1 is the fluorescence intensity of BBOT in the 1:1 inclusion complex, while K_1 is the association constant of the 1:1 inclusion complex.

However, when the concentration of BBOT increases, no reasonable results can be obtained using the models of simple inclusion complexes such as 1:1, 1:2 types or the coexisting of the two, which suggests the formation of a structure different from that of simple inclusion complexes. In this condition, the solution of BBOT-β-CD is a little turbid, while individual solutions of β-CD and BBOT are clear, indicating the existence of large particles. The similar phenomenon has also been observed in PBD-β-CD and PBD-γ-CD solutions, which is the evidence for the existence of the nanotube and secondary assembly [13, 14, 26, 31]. In the present study, the nanotube and secondary assembly of β-CD may

also be formed at higher concentration of BBOT.

The fluorescence anisotropy of BBOT (2×10^{-6} M) upon the addition of β-CD is shown in Figure 4(a). As the solution is not clear, it is necessary to correct the observed anisotropy value that may be affected by light scattering of large particles in the solution. In our previous work, the fluorescence anisotropy of the turbid solution with PBD and β-CD was corrected and the deviation between the actual anisotropy value r', which is not affected by light scattering, and the observed anisotropy r_{obs} was calculated [31, 40, 41]. For BBOT-CD systems, the fluorescence anisotropy of BBOT is corrected in the same way. $(r'\text{-}r_{obs})/r'$ is obtained by the following equation

$$\left(r'-r_{obs}\right)/r'=\left(3-3T\right)/\left(3+7T\right) \tag{3}$$

where T is the total effective fractional transmission at the excitation and emission wavelengths. $(r'\text{-}r_{obs})/r'$ is proportional to the absorbance A [40] and the observed proportionality constant k for the system is 0.713 ± 0.001 (see the inset of Figure 4(a)). r' is obtained by eq. (4).

$$\left(r'-r_{obs}\right)/r'=k\times A \tag{4}$$

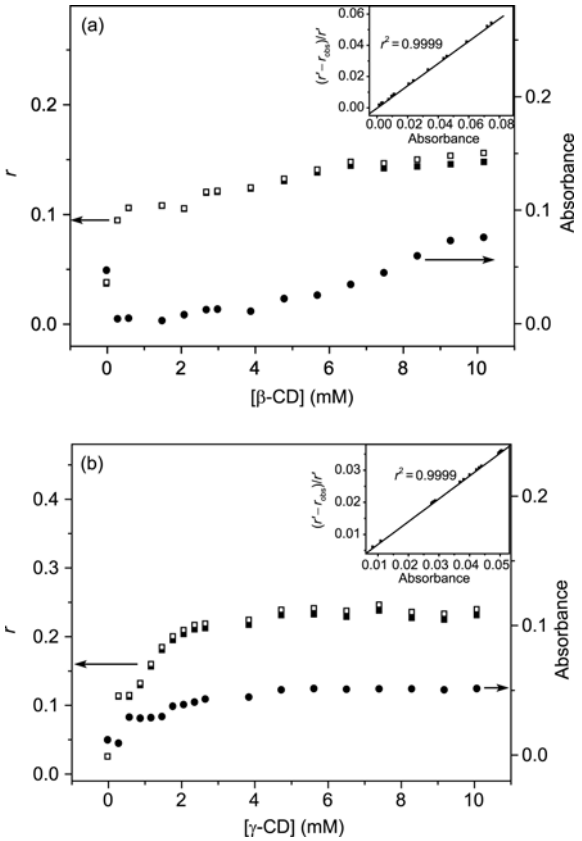

Figure 4 Absorbance value (filled circle), corrected (open square) and observed (filled square) fluorescence anisotropy of BBOT in aqueous solutions of CDs at various concentrations. (a) β-CD; (b) γ-CD ([BBOT] = 2×10^{-6} M, the inset is the dependence of $(r'\text{-}r_{obs})/r'$ of BBOT vs. absorbance in aqueous solutions of β-CD and γ-CD at various concentrations.

where A represents the absorbance.

The r' value of BBOT in 10 mM β-CD is 0.155 while it is only 0.037 for BBOT in pure water, which implies the rotation of BBOT is largely limited in the rigid nanotube.

3.1.3 The interaction of BBOT with γ-CD

In order to study the interaction of BBOT with γ-CD, the models of the simple inclusion complex and combination of several inclusion complexes are applied. However, no reasonable results can be obtained at any concentration of BBOT. Moreover, a red-shift of BBOT occurs after the addition of γ-CD, which results from the overlapping of BBOT molecules in comparatively large cavity of γ-CD. It suggests that γ-CD may form nanotubes even when the concentration of BBOT is comparatively low. The larger r value of BBOT in 10 mM γ-CD indicates the formation of nanotubes (Figure 4(b)).

3.2 The fluorescence image and TEM

Fluorescence microscopy produces sufficient contrast to the background to image the micrometer-sized rods (where the rod is bright relative to the background) in the system of BBOT-β-CD and BBOT-γ-CD (Figures 5(a) and 5(b)). If only pure CD assemblies exist, imaging rods cannot be observed with fluorescence microscopy for pure β-CD is non-fluorescent. Therefore, it is indicated that BBOT exists in the nanotubes of BBOT-β-CD and BBOT-γ-CD. However, such rods are not observed in the aqueous solutions of BBOT-α-CD, confirming that α-CD nanotube cannot be formed with the help of BBOT. The rodlike structures are observed with TEM as illustrated in Figure 6(a). Furthermore, a high-resolution TEM (HRTEM) micrograph shows that the rod as a whole is actually assembled by a lot of smaller nanotubes in a stack way layer by layer (Figure 6(b)). These results further certify the formation of the nanotube and secondary assembly [31].

3.3 Time-resolved fluorescence spectroscopy

The fluorescence lifetimes of BBOT in pure water, in aqueous solutions of α-, β- and γ-CD were measured (Table 1).

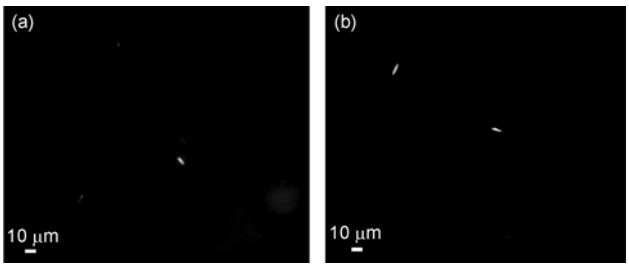

Figure 5 Fluorescence image of the micrometer-sized rodlike structure. (a) BBOT-β-CD; (b) BBOT-γ-CD.

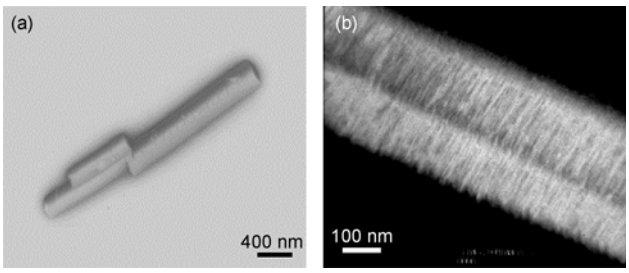

Figure 6 Micrographs of the micrometer-sized rodlike structure of the β-CD secondary assembly induced by BBOT (a) TEM; (b) HRTEM.

Table 1 Fluorescence lifetimes of BBOT in pure water and aqueous solutions of α-, β-, and γ-CD [a)]

Medium	τ_1 (ns)	B_1	τ_2 (ns)	B_2	χ^2
Pure water	1.01 ± 0.01	0.23	3.88 ± 0.02	0.77	1.18
α-CD	0.88 ± 0.01	0.44	2.78 ± 0.03	0.56	1.22
β-CD	1.44 ± 0.01	0.67	3.27 ± 0.04	0.33	1.06
γ-CD	2.22 ± 0.01	0.09	8.90 ± 0.09	0.91	1.13

a) [BBOT] = 2×10^{-6} M, [CD] = 10 mM. B_i is a preexponential factor representing the fractional contribution to the time-resolved decay of the component with a lifetime τ_i, $I(t) = \sum_i B_i e^{-t/\tau_i}$

The shorter lifetime of BBOT in pure water is attributed to the monomer of BBOT and the longer one is attributed to the possible aggregates of BBOT. As for BBOT in CDs, the shorter lifetimes are attributed to the free species of BBOT in aqueous solutions and the longer ones correspond to BBOT in the inclusion complex and nanotubes. Though BBOT can induce β- and γ-CD to form nanotubes, the fluorescence lifetime of BBOT in γ-CD nanotube is much longer than that in the β-CD nanotube. Considering this, the difference of the BBOT molecule array in the two nanotubes is deduced. Because of the larger size of γ-CD, two BBOT molecules could mostly overlap in the same cavity of γ-CD and an excimer is formed. For the relatively small cavity of β-CD, the BBOT molecule hardly overlaps and is arrayed linearly. The formation of the excimer results in a very long lifetime of BBOT in the γ-CD nanotube, which is analogical to the interaction of naphthalene with β-CD. When the concentration of naphthalene is high, the dimer of the 2:2 inclusion complex with β-CD is formed and the fluorescence lifetime of naphthalene is 90.7 ns. It is much longer than 60.9 ns, which is the lifetime of the 1:1 inclusion complex at lower concentration of naphthalene [42]. The result can be further confirmed by the excimer of fluorescence spectra of BBOT in γ-CD aqueous solution (Figure 3(c)).

It can be concluded that the array of BBOT in the β- and γ-CD nanotubes is different. As for the former, BBOT hardly overlaps and arrays linearly. In the nanotube of BBOT-γ-CD, BBOT molecules array linearly and overlap to a great extent.

3.4 DLS measurement

In our previous report, DLS measurement was used to study the formation of the nanotube and secondary assembly. As for the systems of PBD-β-CD and PBD-γ-CD, where the nanotubes can be formed, a new peak with mean hydrodynamic radius around 10 nm exists, which is similar to the phenomenon of DPB-γ-CD [29, 31]. As for the systems where the nanotubes cannot be formed, the new peak will not exist. As a result, the formation of CD nanotubes can be further certified by DLS measurement.

Here, the components of BBOT-β-CD and BBOT-γ-CD systems were also studied by DLS. For comparison, the system of BBOT-α-CD was also measured (Figure 7). A mean hydrodynamic radius of 0.6–0.8 nm is attributed to the monomeric CDs and that around 60–100 nm corresponds to incompact CD aggregates [43]. According to the method suggested by Gonzalez-Gaitano *et al.* for spherical models [43], mass contributions of BBOT-CD systems are calculated (Table 2). The DLS result of the BBOT-α-CD system, where a simple inclusion complex is formed, is approximate to that of α-CD itself [29]. For the systems of BBOT-β-CD and BBOT-γ-CD, except for peaks of monomeric and aggregated CDs, a peak with mean hydrodynamic radius around 10 nm appears. As the secondary assembly has been removed by 0.2 μm filters, the peak is attributed to the intermediate in the development process of the secondary assembly of BBOT-β-CD and BBOT-γ-CD nanotube [44].

3.5 The effect of pH on nanotubes and secondary assembly

It has been reported that hydrogen bonds, hydrophobic effect and van der waals force are significant to the formation of cyclodextrin nanotubes [14–16, 25, 27, 31, 45]. The proton dissociation constant of β-CD is 12.20 [46]. When the pH of the solution is higher than 12.20, OH on the rim of β-CD would become O^- and block the formation of hydrogen

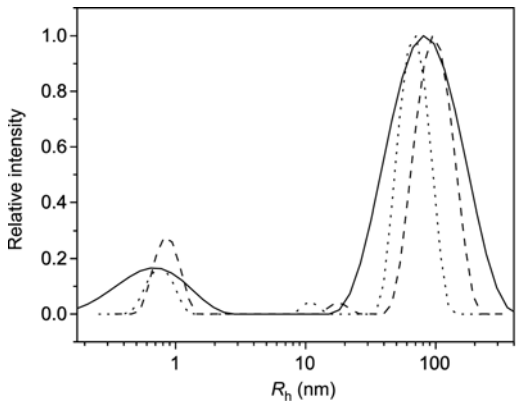

Figure 7 DLS results of the aqueous solutions of BBOT-α-CD (solid line), BBOT-β-CD (dotted line), and BBOT-γ-CD (dashed line) treated with 0.2 μm filters ([BBOT] = 2×10^{-6} M, [CD] = 10 mM).

Table 2 Mean hydrodynamic radius (R_h), correlative intensity (I) and mass (M) contributions of various components in the aqueous solutions of CDs and BBOT-CDs [a)]

Samples	R_{h1} (nm)	I_1 (%)	M_1 (%)	R_{h2} (nm)	I_2 (%)	M_2 (%)	R_{h3} (nm)	I_3 (%)	M_3 (%)
α-CD [b)]	0.6 ± 0.1	6.68	99.9989	/	/	/	64.4 ± 0.5	93.32	0.0011
BBOT-α-CD	0.7 ± 0.1	7.21	99.9981	/	/	/	61.6 ± 0.3	92.79	0.0019
β-CD [b)]	0.8 ± 0.1	14.02	99.9998	/	/	/	114.7 ± 0.4	85.98	0.0002
BBOT-β-CD	0.7 ± 0.2	12.40	99.9951	10.8 ± 0.1	1.90	0.0042	68.0 ± 0.2	85.70	0.0007
γ-CD [b)]	0.7 ± 0.2	3.19	99.9977	/	/	/	76.7 ± 0.5	96.81	0.0023
BBOT-γ-CD	0.8 ± 0.2	15.47	99.9988	17.9 ± 0.1	1.57	0.0009	96.4 ± 0.3	82.96	0.0003

a) [BBOT] = 2×10^{-6} M, [CD] = 10 mM. b) Taken from ref. [29].

bonds between adjacent CDs. Therefore, the effect of pH on the r value of BBOT in β-CD solutions could be used to certify the significance of hydrogen bonds. As shown in Figure 8, the r value of BBOT is almost constant when pH is lower than 13, when the pH value is adjusted to 13, the r value descends greatly, which indicates the nanotube and secondary assembly cannot be formed in the condition. Consequently, it is certified that the hydrogen bond is crucial for the formation of CD nanotubes and secondary assemblies induced by BBOT.

3.6 Structural feature and mechanism of the nanotube and secondary assembly

In our previous report, the structural feature of the PBD-β-CD nanotube and secondary assembly was studied by the measurement of density and fluorescence microscopy. It was concluded that the occupied and empty β-CD nanotubes construct the micrometer-sized secondary assembly together, where most of the β-CD nanotubes are empty and only a few β-CD nanotubes are occupied by PBD [31].

As for BBOT-β-CD, similar methods are used to characterize the structural feature. The solution of BBOT (2×10^{-6} M)-β-CD (10 mM) is centrifuged at a high speed (10000 rpm) and the density of the supernatant fluid is measured at 25 °C. According to the linear relationship between the density of β-CD aqueous solution and its concentration at 25 °C, the concentration of β-CD in the supernatant fluid is estimated to be 5.93 mM, indicating that the moles of β-CD are much larger than that of BBOT in the secondary assembly. Together with the results of fluorescence microscopy, the structure of the secondary assembly is similar to that of PBD-β-CD. Among the secondary assembly, the β-CD nanotubes occupied by BBOT are the minority and the empty β-CD nanotubes which are not occupied by BBOT are the majority.

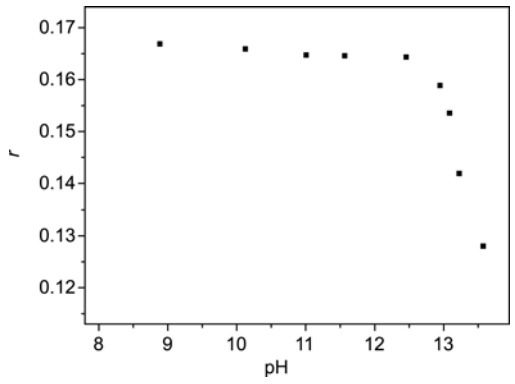

Figure 8 Fluorescence anisotropy of BBOT in the presence of 10 mM β-CD as a function of pH.

Based on the above results and the mechanism of PBD-β-CD nanotubes and secondary assembly in previous reports [31], the probable formation mechanism of BBOT-β-CD nanotubes and secondary assemblies is as follows: when a small amount of BBOT is added into β-CD aqueous solution, a 1:1 inclusion complex forms mainly due to the hydrophobic interaction between BBOT and β-CD. With the concentration of BBOT increasing, except that one molecule is complexed by one β-CD，the segment of the molecules outside the β-CD cavity could enter another cavity of the inclusion complex. Due to the "bridge" effect of BBOT and the hydrogen-bonding between hydroxyl groups of β-CD molecules, the nanotube of β-CD occupied by BBOT is formed. This kind of nanotubes acts as a center for the aggregation of β-CD to form the empty nanotubes. The occupied and empty nanotubes make up of the micrometer-sized secondary assembly together.

4 Conclusions

As is shown above, the interaction patterns of BBOT with α-, β-, γ-CD are different. BBOT and α-CD can form a 1:2 inclusion complex. BBOT can form a 1:1 inclusion complex with β-CD at comparatively low concentration of the molecule. Once the concentration of BBOT increases, it induces β-CD to construct nanotubes and a micrometer-sized rod-like structure by further assembly. It has been demonstrated that the hydrogen bond of adjacent CDs is crucial for the formation of the nanotube and secondary assembly. As for γ-CD, the nanotube and secondary assembly can be formed at any concentration of BBOT studied here. In γ-CD nanotubes, BBOT molecules mostly overlap in the same cavity of γ-CD.

This work was supported by the National Natural Science Foundation of China (29901001 and 20871009).

1 Harada A, Takashima Y, Yamaguchi H. Cyclodextrin-based supramolecular polymers. *Chem Soc Rev*, 2009, 38: 875–882
2 He YF, Fu P, Shen XH, Gao HC. Cyclodextrin-based aggregates and characterization by microscopy. *Micron*, 2008, 39: 495–516
3 Wenz G, Han BH, Muller A. Cyclodextrin rotaxanes and polyrotaxanes. *Chem Rev*, 2006, 106: 782–817
4 Wylie RS, Macartney DH. Self-assembling metal rotaxane complexes of α-cyclodextrin. *J Am Chem Soc*, 1992, 114: 3136–3138
5 Harada A, Li J, Kamachi M. The molecular necklace – A rotaxane containing many threaded α-cyclodextrins. *Nature*, 1992, 356: 325–327
6 Luttringhaus A, Cramer F, Prinzbach H. Einschlussversuche und cyclisationsversuche an langkettigen dithiolen. *Angew Chem Int Ed*, 1957, 69: 137–137
7 Harada A, Li J, Kamachi M. Synthesis of a tubular polymer from threaded cyclodextrins. *Nature*, 1993, 364: 516–518
8 Hernandez-Pascacio J, Garza C, Banquy X, Diaz-Vergara N, Amigo A, Ramos S, Castillo R, Costas M, Pineiro A. Cyclodextrin-based self-assembled nanotubes at the water/air interface. *J Phys Chem B*, 2007, 111: 12625–12630
9 Liu Y, Yang ZX, Chen Y, Song Y, Shao N. Construction of a long cyclodextrin-based bis(molecular tube) from bis(polypseudorotaxane) and its capture of C-60. *ACS Nano*, 2008, 2: 554–560
10 Park C, Im MS, Lee S, Lim J, Kim C. Tunable fluorescent dendron-cyclodextrin nanotubes for hybridization with metal nanoparticles and their biosensory function. *Angew Chem Int Ed*, 2008, 47: 9922–9926
11 Rodriguez J, Semino R, Laria D. Building up nanotubes: Docking of "Janus" cyclodextrins in solution. *J Phys Chem B*, 2009, 113: 1241–1244
12 Ohira A, Sakata M, Taniguchi I, Hirayama C, Kunitake M. Comparison of nanotube structures constructed from α-, β-, and γ-cyclodextrins by potential-controlled adsorption. *J Am Chem Soc*, 2003, 125: 5057–5065
13 Agbaria RA, Gill D. Extended 2,5-diphenyloxazole-γ-cyclodextrin aggregates emitting 2,5-diphenyloxazole excimer fluorescence. *J Phys Chem*, 1988, 92: 1052–1055
14 Agbaria RA, Gill D. Noncovalent polymers of oxadiazole derivatives induced by γ-cyclodextrin in aqueous-solutions – Fluorescence study. *J Photochem Photobiol A: Chem*, 1994, 78: 161–167
15 Li G, McGown LB. Molecular nanotube aggregates of β-cyclodextrins and γ-cyclodextrins linked by diphenylhexatrienes. *Science*, 1994, 264: 249–251
16 Pistolis G, Malliaris A. Nanotube formation between cyclodextrins and 1,6-diphenyl-1,3,5-hexatriene. *J Phys Chem*, 1996, 100: 15562–15568
17 Girardeau TE, Leisen J, Beckham HW. Chain dynamics of poly (oxyethylene) in nanotubes of α-cyclodextrin by solid-state ^{2}H NMR. *Macromol Chem Phys*, 2005, 206: 998–1005
18 Agnew KA, McCarley TD, Agbaria RA, Warner IM. Phase-transition pattern of 2,5-diphenyloxazole/γ-cyclodextrin (PPO/γ-CD) self-assembly aggregates. *J Photochem Photobiol A: Chem*, 1995, 91: 205–210
19 Das P, Chakrabarty A, Haldar B, Mallick A, Chattopadhyay N. Effect of cyclodextrin nanocavity confinement on the photophysics of a β-carboline analogue: A spectroscopic study. *J Phys Chem B*, 2007, 111: 7401–7408
20 Tormo L, Organero JA, Douhal A. Effect of nanocavity confinement on the relaxation of anesthetic analogues: Relevance to encapsulated drug photochemistry. *J Phys Chem B*, 2005, 109: 17848–17854
21 El-Kemary M, Organero JA, Santos L, Douhal A. Effect of cyclodextrin nanocavity confinement on the photorelaxation of the cardiotonic drug milrinone. *J Phys Chem B*, 2006, 110: 14128–14134
22 Douhal A. Ultrafast guest dynamics in cyclodextrin nanocavities. *Chem Rev*, 2004, 104: 1955–1976
23 Shimomura T, Akai T, Abe T, Ito K. Atomic force microscopy observation of insulated molecular wire formed by conducting polymer and molecular nanotube. *J Chem Phys*, 2002, 116: 1753–1756
24 Roy D, Mondal SK, Sahu K, Ghosh S, Sen P, Bhattacharyya K. Temperature dependence of anisotropy decay and solvation dynamics of coumarin 153 in γ-cyclodextrin aggregates. *J Phys Chem A*, 2005, 109: 7359–7364
25 Wen XH, Guo M, Liu ZY, Tan F. Nanotube formation in solution between β-cyclodextrin and cinchonine. *Chem Lett*, 2004, 33: 894–895
26 Zhang CF, Shen XH, Gao HC. Studies on the nanotubes formed by 2-phenyl-5-(4-diphenylyl)1,3,4-oxadiazole and cyclodextrins. *Chem Phys Lett*, 2002, 363: 515–522
27 Zhang CF, Shen XH, Gao HC. Studies on the formation of cyclodextrin nanotube by fluorescence and anisotropy measurements. *Spectrosc Spectr Anal*, 2003, 23: 217–220
28 Wu AH, Shen XH, Gao HC. Cyclodextrin nanotube induced by 4,4'-bis(2-benzoxazolyl) stilbene. *Int J Nanosci*, 2006, 5: 213–218
29 Wu AH, Shen XH, He YK. Investigation on γ-cyclodextrin nanotube induced by *N,N'*-diphenylbenzidine molecule. *J Colloid Interf Sci*, 2006, 297: 525–533
30 Cheng XL, Wu AH, Shen XH, He YK. The formation of cyclodextrin nanotube induced by POPOP molecule. *Acta Phys-Chim Sin*, 2006, 22: 1466–1472
31 Wu AH, Shen XH, He YK. Micrometer-sized rodlike structure formed by the secondary assembly of cyclodextrin nanotube. *J Colloid Interf Sci*, 2006, 302: 87–94
32 Sowmiya M, Purkayastha P, Tiwari AK, Jaffer SS, Saha SK. Characterization of guest molecule concentration dependent nanotubes of β-cyclodextrin and their secondary assembly: Study with trans-2-[4(dimethylamino)styryl]benzothiazole, a TICT-fluorescence probe. *J Photochem Photobiol A: Chem*, 2009, 205: 186–196
33 Jaffer SS, Saha SK, Purkayastha P. Fragmentation of molecule-induced γ-cyclodextrin nanotubular suprastructures due to drug dosage. *J Colloid Interf Sci*, 2009, 337: 294–299
34 Kim JS, Seo BW, Gu HB. Exciplex emission and energy transfer in white light-emitting organic electroluminescent device. *Synth Met*, 2003, 132: 285–288
35 Tian WJ, Wu F, Zhang LQ, Zhang BW, Cao Y. Light emission from exciplex of organic electroluminescent device. *Synth Met*, 2001, 121: 1725–1726
36 Shen XH, Belletete M, Durocher G. Interactions between a surface- active cationic 3H-indole molecular probe and β-cyclodextrin. Design of a novel type of rotaxane. *Chem Phys Lett*, 1999, 301: 193–199
37 Shen XH, Belletete M, Durocher G. Spectral and photophysical studies of the 1:3 (guest/host) rotaxane-like inclusion complex formed by a 3*H*-indole and β-cyclodextrin. *J Phys Chem B*, 1998, 102: 1877–1883
38 Shen XH, Belletete M, Durocher G. Quantitative study of the hydrophobic interaction mechanism between urea and molecular probes used in sensing some microheterogeneous media. *J Phys Chem B*, 1997, 101: 8212–8220
39 Shen XH, Belletete M, Durocher G. Studies of the inclusion complexation between a 3*H*-indole and β-cyclodextrin in the presence of urea, sodium dodecyl sulfate, and 1-propanol. *Langmuir*, 1997, 13: 5830–5836
40 Teale FWJ. Fluorescence depolarization by light-scattering in turbid solutions. *Photochem Photobiol*, 1969, 10: 363–374
41 Lentz BR, Moore BM, Barrow DA. Light-scattering effects in the measurement of membrane microviscosity with diphenylhexatriene. *Biophys J*, 1979, 25: 489–494
42 Grabner G, Rechthaler K, Mayer B, Kohler G, Rotkiewicz K. Solvent influences on the photophysics of naphthalene: Fluorescence and triplet state properties in aqueous solutions and in cyclodextrin complexes. *J Phys Chem A*, 2000, 104: 1365–1376
43 Gonzalez-Gaitano G, Rodriguez P, Isasi JR, Fuentes M, Tardajos G, Sanchez M. The aggregation of cyclodextrins as studied by photon correlation spectroscopy. *J Incl Phenom Macrocycl Chem*, 2002, 44: 101–105
44 He YF. Investigation on inclusion complex of cyclodextrin and secondary assembly of cyclodextrin nanotube. *Doctor Dissertation.* Beijing: Peking University Press, 2008
45 Xia K, Hou TJ, Xu XJ, Shen XH. Molecular modeling of DPH-cyclodextrins nanotube-type aggregate. *Acta Phys-Chim Sin*, 2004, 20: 5–8
46 Li S, Purdy WC. Cyclodextrins and their applications in analytical-chemistry. *Chem Rev*, 1992, 92: 1457–1470